Theoretical Population Biology **52**, 179–197 (1997)
Article No. TP971331

Using Moment Equations to Understand Stochastically Driven Spatial Pattern Formation in Ecological Systems

Benjamin Bolker* and Stephen W. Pacala†

Department of Ecology and Evolutionary Biology, Princeton University, Princeton, New Jersey 08544-1003

Received August 8, 1996

Spatial patterns in biological populations and the effect of spatial patterns on ecological interactions are central topics in mathematical ecology. Various approaches to modeling have been developed to enable us to understand spatial patterns ranging from plant distributions to plankton aggregation. We present a new approach to modeling spatial interactions by deriving approximations for the time evolution of the moments (mean and spatial covariance) of ensembles of distributions of organisms; the analysis is made possible by "moment closure," neglecting higher-order spatial structure in the population. We use the growth and competition of plants in an explicitly spatial environment as a starting point for exploring the properties of second-order moment equations and comparing them to realizations of spatial stochastic models. We find that for a wide range of effective neighborhood sizes (each plant interacting with several to dozens of neighbors), the mean-covariance model provides a useful and analytically tractable approximation to the stochastic spatial model, and combines useful features of stochastic models and traditional reaction-diffusion-like models.

1. INTRODUCTION

The generation of spatial patterns in biological populations and the effect of spatial patterns on ecological interactions are central topics in ecology. Exogenous factors such as topography, distributions of resources, or disturbance can create spatial patterns in natural populations; so can endogenous factors connected to the behavior and ecological interactions of individuals. In this paper we focus on explaining the generation of endogenous spatial patterns by dispersal and competitive interaction between individual plants, and on the feedback of spatial patterns on the dynamics of the population. Local movement and differential survivorship and fecundity of individuals in different surroundings generate the spatial pattern (for example, see Fig. 1); in turn, the spatial pattern affects population dynamics by changing local densities and hence the effective strengths of competitive interactions.

Consider a spatial ecological process where individuals similar to perennial plants can reproduce, dispersing their offspring locally, and die, at rates dependent on their local density. These events occur randomly, but according to well-defined rates, in continuous time. All individuals are identical and stationary once they have dispersed from their parents. For this simple system, any given population will eventually reach a roughly constant mean density; it will also develop a statistically constant spatial pattern (clustering or even spacing), although the details of the pattern will shift randomly over time. Fig. 1 shows a snapshot of a point-process simulation of such a population in continuous two-dimensional space. The snapshot is taken after 40 time steps, enough time for the system to reach a steady-state mean and degree of clustering, although the exact spatial pattern continues to fluctuate. There is clear evidence of a spatial pattern: calculating the variance-to-mean ratio

* E-mail: ben@eno.princeton.edu.
† E-mail: steve@eno.princeton.edu.

0040-5809/97 $25.00

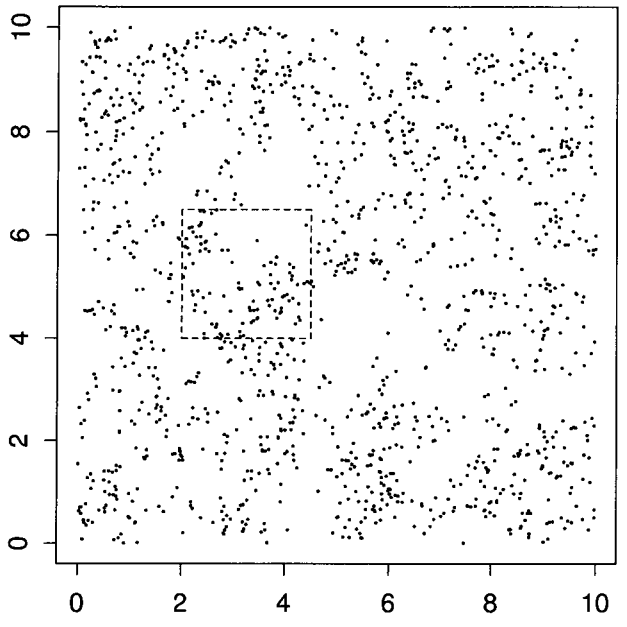

FIG. 1. Snapshot of a point-process simulation in which individuals die at a rate dependent on their local density and disperse their offspring locally. Mean ≈ 14; $\sigma^2/\mu = 5.7$ for a quadrat scale of 2.5 units (sample quadrat shown by dashed square; values of $\sigma^2/\mu > 1$ indicate clustering).

(σ^2/μ) for different-sized quadrats between 1 and 3 gives values between 4 and 6 (σ^2/μ reflects the population density seen by an average individual in a population; values greater than 1 imply clustering). In addition, the spatial clustering has significant effects on the population dynamics, raising the local density experienced by individuals by about 35% and depressing the overall mean density (from that expected in the nonspatial case) by 30%, from 20 to approximately 14 individuals per unit area.

We present an approach to modeling the creation and effects of spatial patterns like that shown in Fig. 1. The point-process simulation used in Fig. 1 uses discrete individuals that give birth and die stochastically in continuous space. Our approach preserves the discreteness of individuals (and hence the demographic stochasticity) and explicit space; it is also analytically tractable. We derive and analyze approximate equations for the evolution of the moments (mean densities and spatial covariances) of ensembles of plant populations over time. Our models naturally produce spatial patterning (spacing and clustering) in straightforward and intuitive ways.

Almost all of the currently popular, analytically tractable models for spatial pattern formation and population dynamics lack two properties of ecological populations. The first property is the presence of discrete individuals and hence of *demographic stochasticity*, the fluctuations caused by the occurrence of random events (birth, death, etc.) in a finite population (Durrett and Levin, 1994b). In a model with demographic stochasticity, the presence of an individual at a particular spot seeds cluster formation in a way that is impossible in continuous-density models. The second property is *local interaction*, which allows the spatial structure seeded by demographic stochasticity to build up over time. Nonspatial models implicitly have infinite interaction ranges. Pseudo-spatial models such as lottery models (Chesson and Warner, 1981; Shmida and Ellner, 1984) do incorporate local and global dispersal, but fail to distinguish any intermediate distances between zero (within-patch interactions) and infinity (between-patch interactions). Durrett and Levin refer to these properties in their paper "The Importance of Being Discrete (and Spatial)" (1994a); interacting particle systems do incorporate both properties, but are at the edge of analytical tractability. Our moment equations also incorporate these properties, in a way that is both easier to handle analytically and easier to match with field data.

The rest of this section briefly reviews three broad classes of current spatial models (continuous-density models, lattice and patch models, and simulation models), focusing on their discreteness and finite-dispersal properties, analytical tractability, and ability to simply generate realistic spatial structure.

Theoretical biologists have used continuous, deterministic models based on partial differential equations (PDEs) to understand the effects of space (Holmes *et al.*, 1994); some examples are diffusion and reaction-diffusion equations (Okubo, 1980; Murray, 1990) and partial integro-differential equations (Levin and Segel, 1982). Pattern-generating mechanisms in PDEs include diffusive instabilities in reaction-diffusion equations (Okubo, 1980), density-dependent diffusion (Mimura, 1981; Mimura *et al.*, 1984), and models with aggregation terms (Levin and Segel, 1982). PDEs are spatial, but not discrete, and as a result do not display the simple clustering behaviors of discrete spatial models.

Spatially structured models encompass all cases where space is broken up into some kind of patch or cell structure; they include everything from pseudo-spatial patch and lottery models where the dynamics within relatively large patches are well-mixed (and often fast) relative to dynamics between patches (Chesson and Warner, 1981; Shmida and Ellner, 1984; Gilpin and Hanski, 1991; Tilman, 1994), to coupled-map, cellular automaton, and interacting particle system models (Solé *et al.*, 1992a, 1992b; Matsuda *et al.*, 1992; Durrett and Levin, 1994b; Durrett and Levin, 1994a; Harada and Iwasa, 1994;

Molofsky, 1994) where the patches tend to be small, close together, and regularly spaced on some kind of lattice. Patch models and lottery models can be discrete, but not fully spatial; as mentioned above, they only make the distinction between local and global interactions, with no intermediate spatial scales. Lattice-based models are discrete and fully spatial but are analytically difficult and can be hard to calibrate to field studies or experiments.

Finally, simulation (often individual-based) models include everything that cannot be fit easily into an analytic framework, but must be simulated on a computer; these models include detailed models of forest succession (Pacala *et al.*, 1996; Urban *et al.*, 1991) and of fruit fly populations (Atkinson and Shorrocks, 1981), among many others (Provencher and Riechert, 1994; Cain *et al.*, 1991; Real *et al.*, 1992; Ford and Diggle, 1981). These models can be enormously flexible, and are often custom designed to be calibrated from field and lab measurements, but are usually impossible to analyze fully, making it hard to understand or generalize the results of a particular simulation model.

Our approach combines continuous space, stochasticity, calibration ability, and analytical tractability in a way that combines some of the best features of standard spatial models. In the following sections we will define a simple spatial model for growth of a single-species perennial plant population, reduce the full stochastic model to two approximate equations for the average mean density and average spatial covariance of stochastic realizations, and explore the model and various extensions.

2. A PLANT-GROWTH MODEL WITH DENSITY-DEPENDENT MORTALITY

To illustrate the derivation of analytically tractable moment equations from a stochastic, individual-based model, we will start with a simple spatial extension of logistic population growth. In the next two sections we will first present the formal definition of a stochastic model for a spatial ecological system (Section 2.1) and then show the time-evolution equations for the mean and approximate spatial covariance (Section 2.2). The technical details of the derivation are given in Appendices A and B. Sections 2.3 and 3 compare the moment equations to the full stochastic system and explore the analytic and ecological consequences of spatial structure. Finally, Section 4 shows some extensions of the model and discusses other work in progress for exploiting the power of moment equations for understanding ecological systems.

2.1. Stochastic Model

To begin with we consider a population of perennial plants growing in a continuous, homogeneous, and infinite spatial arena. We start with the case of density-dependent mortality, where the *per capita* mortality rate increases as a function of local density; we address extensions to other cases (density-dependent fecundity or germination) later (Section 4). The state variable $n(x, t)$ represents the density of plants at position x at time t, which is a sum of Dirac δ functions for a point process: the integral of $n(x, t)$ over some area ω gives the number of plants located within ω at time t (see Table I for notation). Death, reproduction, and dispersal occur randomly in continuous time. The overall mortality rate of a plant at location x at time t is

$$M(x, t) = \mu + \alpha d(x, t), \tag{1}$$

a linear function of local density $d(x, t)$ with slope α and intercept (density-independent mortality) μ (we will discuss situations where mortality is a nonlinear increasing

TABLE I

Symbols Used in Order of Appearance

Symbol	Description (Units)
$M(x, t)$	Overall mortality rate (time^{-1})
μ	Density-independent mortality (time^{-1})
α	Competition parameter (individual^{-1}time^{-1})
$d(x, t)$	Local density (individuals)
$n(x, t)$	Individual density
$U(x)$	Competition kernel
f	Fecundity (time^{-1})
$D(x)$	Dispersal kernel
$r = f - \mu$	Nonspatial max. growth rate (time^{-1})
$K = (f - \mu)/\alpha$	Nonspatial carrying-capacity (individuals)
ω	Box size (length)
Ω	Spatial region
λ_u	Competition scale parameter (length^{-1})
λ_d	Dispersal scale parameter (length^{-1})
$\mathscr{L}(\lambda, x)$	Laplacian kernel
$c(r)$	Spatial covariance at distance r (individuals^2)
$\bar{c}$	Average (competition-weighted) spatial covariance (individuals^2)
$n(t)$	Mean density (individuals)
μ'	Mortality incorporating self-competition (time^{-1})
$\lambda\phi_+, \lambda\phi_-$	Scale parameters of equilibrium covariance (length^{-1})
$\varepsilon = \lambda_u/\lambda_d$	Ratio of competition to dispersal parameter
$\gamma = \mu/f$	1/(maximum lifetime fecundity)
g_+, g_-	Coefficients of Laplacians in equilibrium covariance
g_r, g_i, ϕ_r, ϕ_i	Real and imaginary parts of g_+, ϕ_+
g_c, g_s	Coefficients of cosine and sine parts of equilibrium covariance

function of local density in Section 4). The local density is defined as

$$d(x, t) = \int_{y \in \Omega} U(y - x) n(y, t) = \sum_{\text{all plants}} U(y_i - x) \quad (2)$$

where Ω is the entire space, y_i is the location of the ith plant, and U is the *competition kernel*, a function of distance which determines the strength of competition between two plants a given distance apart (without loss of generality, we normalize U to a probability distribution function (pdf: $\int_{x \in \Omega} U(x) \equiv 1$)).

Each individual reproduces at a constant rate f, leading to a Poisson distribution of births per individual per unit time. Once a seed is produced, it is instantaneously dispersed to a random position a distance z away from its parent with a probability governed by the *dispersal kernel* $D(z)$, another symmetric pdf.

The analogous nonspatial model is logistic growth with exponential growth rate $r = f - \mu$ and carrying capacity $K = r/\alpha$, $dn/dt = rn(1 - n/K)$. As the competition kernel becomes very long-range, the local density approaches a global density and the model becomes effectively nonspatial: even though clustering can and will build up in the system, it will make no difference to the dynamics of the mean density. Local competition and local dispersal combine to generate the special features of this model.

The rates of processes that change $N(x)$, the number of individuals in a small region (of size ω) around x, are:

Process	$\Delta N(x)$	Rate
Death	-1	$N(x)\left[\mu + \alpha \int_{y \in \Omega} U(y - x)\, N(y)\right]$
Birth	$+1$	$f\omega \int_{y \in \Omega} D(y - x)\, N(y)$

(3)

Simulations of this model (Fig. 2) keep track of spatial positions in continuous (floating-point) space and use a small-step, discrete-time approximation. (A more rigorous and possibly more efficient approach would update the state of the population asynchronously by picking exponentially distributed random variates for the time between events (R. Durrett and L. Buttel, personal communication).) All simulations reported here use periodic boundary conditions. Fig. 2 shows one such realization in one spatial dimension, with space on the y-axis and time moving to the-right on the x-axis: each continuous horizontal line represents the "life-line" of a single plant.

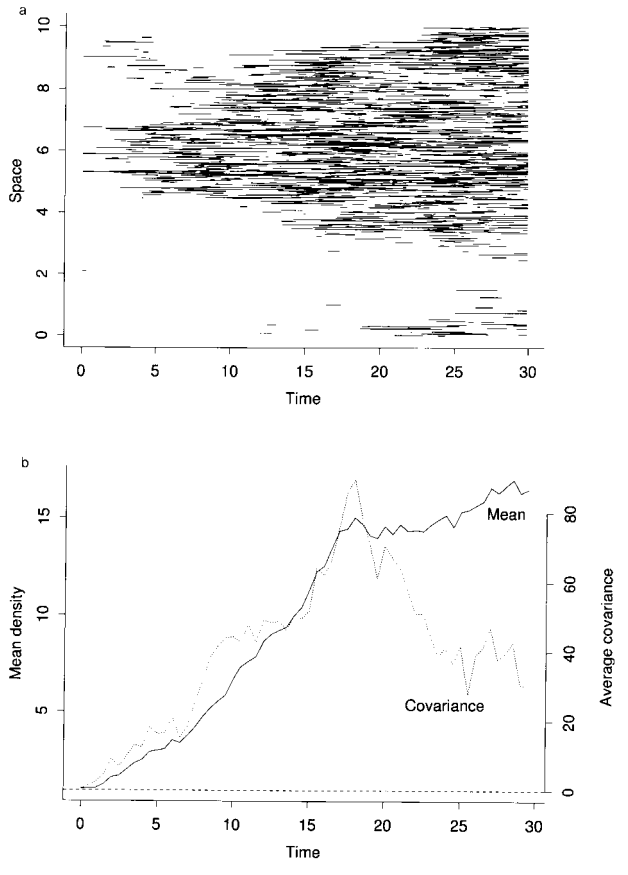

FIG. 2. Stochastic simulation results. Parameters are: $f = 0.8$, $\mu = 0.4$, $\alpha = 0.02$; $U(x) = \lambda_u \exp(-\lambda_u |x|)/2$, $D(x) = \lambda_d \exp(-\lambda_d |x|)/2$, $\lambda_u = \lambda_d = 1.0$. Length $= 50$, $n(0) = 1$. (a) Location (y-axis) and lifespan (horizontal length) of individual plants in the simulation (only a segment of the simulation is shown for clarity). (b) Summary measures of the simulation shown in (a): mean density (left-hand axis) of plants and average covariance ($\bar{c} = \int U(r)\, c(r)\, dr$, right-hand axis) over time.

This particular realization uses *Laplacian*, or bilateral exponential, competition and dispersal kernels; $U(x) \propto \exp(-\lambda_u |x|)$, $D(x) \propto \exp(-\lambda_d |x|)$; we define $\mathscr{L}(\lambda, x) \equiv \lambda/2 \exp(-\lambda |x|)$, sometimes just referring to $\mathscr{L}(\lambda)$ for brevity. Although the derivation of the moment equations will work with arbitrary competition and dispersal kernels, Laplacian kernels are particularly simple to analyze, as shown below (Section 3; Slatkin, 1973). The importance of space depends on the number of individuals in an average neighborhood; as the number of individuals grows large, the effects of demographic stochasticity diminish and the system approaches the behavior of the nonspatial system. The neighborhood population size scales with the nonspatial carrying capacity, $K = (f - \mu)/\alpha$, and the scales of the competition and dispersal kernels. In this case K equals 20 ($f = 0.8$; $\mu = 0.4$; $\alpha = 0.02$). We set $\lambda_u = \lambda_d = 1.0$, and the

standard deviation of an exponential distribution is $\sigma = 1/\lambda$, so the average size of a competitive neighborhood (looking to both the left and the right along the one-dimensional habitat) is approximately $2/\lambda_u$, or 2 spatial units, and the average number of competitive neighbors in a randomly distributed population is $2 \times 20 = 40$.

Figure 2b shows the growth of the mean density and clustering in the simulation over time. The *spatial autocovariance*, or covariance for short, is a natural summary of spatial pattern. The covariance

$$c(x-y) = \langle (n(x) - \bar{n}) \cdot (n(y) - \bar{n}) \rangle \tag{4}$$

(where $\langle \cdot \rangle$ denotes an expectation) measures the association between points a given distance apart. To summarize the spatial pattern even further, we take the average covariance weighted by the competition kernel:

$$\bar{c} = \int_{\substack{r \in \Omega \\ r \neq 0}} U(r)\, c(r) dr. \tag{5}$$

This weighted average of the covariance is effectively the variance of the system, analogous to the interpatch variance in a discrete-space model. (Since the integral in (5) excludes zero—the individual's own position—this variance excludes the variability caused by the discrete nature of individuals, which is equal to the mean and which we call the *Poisson variance*. The total variance of the system including Poisson variance (proportional to the average neighborhood density near a plant counting the plant itself) is $\bar{c} + \bar{n}$.)

The weighted covariance divided by the mean density ($\bar{c}/\bar{n}$) represents the extra number of competitive neighbors per individual expected over the mean because of clustering (or the lower number of neighbors, in the case of a regular pattern); using the total variance instead gives $\bar{c}/\bar{n} + 1$, which counts the individual as part of its own neighborhood. Dividing covariance by the mean squared ($\bar{c}/\bar{n}^2$, analogous to the square of the coefficient of variation) gives the increase or decrease in neighborhood density proportional to the mean. One can construct analogues of all of the classical clustering indices, such as Lloyd's mean crowding ($\sigma^2/\bar{n} + \bar{n} - 1$), by substituting $\bar{c} + \bar{n}$ for the variance. The weighted covariance $\bar{c}$ will appear naturally in the dynamical equations discussed in Section 2.2 for the mean and covariance.

In a nonspatial model (in the limit of infinitely long-range competition and dispersal), the mean follows a logistic growth curve and the covariance fluctuates around zero. In the spatial model shown here the mean density still increases roughly logistically, but the system develops positive average covariance; the population self-organizes into a clustered distribution.

2.2. Moment Equations

By taking expected values of the population growth process described above, we can reduce the stochastic process defined in Eq. (3) to a pair of moment equations, an ordinary differential equation describing the average density (first moment) and an integro-partial differential equation describing the average spatial covariance across all realizations (second moment). The derivations are presented in Appendices A and B.

2.2.1. *Mean density equation.* The equation for the mean density n is

$$\frac{dn(t)}{dt} = n(t)(f - \mu - \alpha n(t)) - \alpha U(0)\, n(t) - \alpha \int_{r \in \Omega} U(r)\, c(r, t)\, dr, \tag{6}$$

where $n(t)$ is the mean density at time t and $c(r, t)$ is the *spatial covariance density* at lag r and time t (we switch notation here from the local density in a realization, $n(x, t)$, to the expected mean density, $n(t)$—from now on we will only consider the mean density). The covariance is a function of the lag r; its effect on the mean is through the competition-weighted average $\bar{c}$.

Equation 6 consists of the mean-field (nonspatial) derivative $n(f - \mu - \alpha n)$ and two correction terms. The nonspatial term is equivalent to nonspatial logistic growth, with intrinsic rate of increase $r = f - \mu$ and carrying capacity $K = \alpha/r$. As in the logistic equation, population growth rates are increased by high fecundity (f) and decreased by high density-independent (μ) and density-dependent (α) mortality rates.

The first correction term ($\alpha U(0)\, n$) represents the effect of self-competition; we call it the "Poisson term" because it will be present even when a population of discrete individuals is Poisson-distributed in space. If all individuals were randomly distributed in space ($c(r) = 0$ for all r, so that the last term in (6) was equal to zero), the mean density would grow according to the logistic growth equation, but with the density-independent mortality rate increased by self-competition. The Poisson term only occurs when the population consists of discrete individuals; Durrett and Levin (1994a) and Pacala (1986) have both used this correction term to account for the effects of discrete individuals. If we choose, we can

either remove the Poisson term from the model (by setting $U(0) \equiv 0$) or incorporate it into the baseline mortality μ, setting $\mu' \equiv \mu + \alpha U(0)$; operationally, any measurement of the mortality rate of a plant growing in isolation will always include the self-competition effect. (The Poisson term will have more significant effects when competition has a non-linear effect on mortality.)

The second correction term ($\alpha\bar{c}$) is the correction for spatial structure, the difference between the overall average density and the local density, or between the point-centered and plant-centered mean densities. As discussed in Section 2.1, $\bar{c}$ is like a crowding index; Eq. (6) shows that $\bar{c}$ arises naturally from the derivation of the moment equations. Growth rates depend on the neighborhood density; thus if plants are clustered ($\bar{c} > 0$) growth rates will be lower than expected from the non-spatial term because individuals are more crowded and experience more competition than would be expected from the mean density. Conversely, if plants are regularly spaced ($\bar{c} < 0$), growth rates will be higher than expected. Poisson-distributed populations ($\bar{c} = 0$) grow exactly as expected from the mean density, with the exception of the self-competition term.

Considering just the mean equation (Eq. (6)), the moment equations are essentially a "neighborhood model" (Pacala and Silander, 1985; Pacala, 1986; Pacala and Silander, 1987), where the growth term is modified by information about neighborhood density. Neighborhood models incorporate the effects of spatial structure on population dynamics. Where we go beyond neighborhood models is to consider the evolution of spatial structure itself, and the feedback between spatial structure and dynamics, by deriving an equation for the time evolution of the spatial covariance of the population.

2.2.2. *Covariance density equation.* The equation for the time evolution of the spatial covariance is an integro-partial differential equation because covariance is a function of both time and space or spatial lag, the distance between two points. The major difference between the derivations of the mean equation and the covariance equation (besides the complexity of the expressions involved) is that, just as a covariance term appears in the mean equation because of an interaction between plants and their neighbors, a *third moment* term appears in the covariance equation because of a three-way interaction between a plant, its neighbor, and its neighbor's competitor. Similarly, the third-moment equation (if we were to derive it) would have fourth-moment terms in it. Every stochastic spatial model involves an infinite series of moments; various strategies, from moment-generating functions (Bartlett, 1956) to "moment closure" approximations (Whittle, 1957; Grenfell *et al.*, 1995), have been developed to approximate or otherwise deal with this series. We chop off the chain of moments by assuming that the third central moment is negligible; this assumption is the foundation of our approach, and we are working to extend the methods of Durrett and Neuhauser (Durrett and Neuhauser, 1994) to generate formal proofs that this approximation works in various limits (Pacala and Neuhauser, in prep.). In practice, the naïve truncation approach seems to work remarkably well; we will explore the accuracy of the approximation in Section 2.3 and discuss the meaning and measurement of third moments below in Section 5.

A fair amount of algebra (Appendix B) gives the approximate equation governing the time evolution of the covariance

$$\begin{aligned}\frac{\partial c(r)}{\partial t} = 2 \times [& -\mu' c(r) + f\{(D * c)(r) + nD(r)\} \\ & - \alpha n\{(U * c)(r) + nU(r) + c(r)\} \\ & - \alpha U(r)\, c(r)\,], \end{aligned} \tag{7}$$

where $*$ denotes a *convolution*:

$$(a * b)(y) \equiv \int_{y \in \Omega} a(x)\, b(x - y)\, dx. \tag{8}$$

While the covariance equation (Eq. (7)) is more complicated than the equation for the mean density, its terms are easy to interpret in terms of pattern formation and disappearance. The first term inside the square brackets represents the decrease of any pattern (clustering or spacing) towards randomness by density-independent mortality; the second term represents clustering (growth of positive covariance) by reproduction and local dispersal; and the last two terms represent thinning (growth of negative covariance) by density-dependent mortality.

Equation 7 also shows that the moment equations allow the growth of pattern in a homogeneous environment, starting from a Poisson distribution of plants ($c(r) = 0$ for all $r > 0$), driven by the discrete nature of individuals. In a Poisson distribution, the time derivative of the covariance at lag r (Eq. (7)) is $2n(fD(r) - \alpha U(r))$, which will be positive or negative depending on the balance between competition and the combination of fecundity and dispersal, but will only be zero for all possible lags under highly non generic conditions. Under most circumstances, spatial pattern (non-zero covariance) will develop spontaneously in the population.

The terms that depend on n but not on $c(r)$ in Eq. (7), which generate spontaneous pattern formation, arise

from the inevitability of finding a plant at zero lag (at its own position). This self-interaction leads to a variance term, which is formally a Dirac δ function in the covariance; the variance term creates instability in a spatially homogeneous system, generating seeds for pattern formation. In classical reaction-diffusion equations, one typically tests the homogeneous equilibrium state ($n(x)$ everywhere constant) for stability to small perturbations at different wavelengths (Murray, 1990); we can show (Appendix C) that the deterministic analogue of our model has a homogeneous equilibrium which is always stable against perturbations at any wavelength, and so never generates a pattern spontaneously. In the moment equations the n-driven terms result in a homogeneous state $\{n = (f-\mu)/\alpha,\ c(x) = 0 \text{ for all } x\}$ that is not even an equilibrium for general choices of parameters, let alone a stable equilibrium.

2.3. Comparison of Stochastic and Moment Equation Models

The key assumption in deriving the covariance equation is that the third-moment terms are negligible. To see whether this approximation really works, we will compare the results of stochastic simulations (which fully implement the individual-based stochastic model defined in Section 2.1) with the predictions of the moment equations.

How well, and over what range of parameters, do the predictions of the second-order moment equations match the full stochastic system? The most important parameters are the spatial scale parameters of the kernels, λ_d and λ_u. As the spatial scale becomes large, the errors in the moment equations become small—but so does the difference between the spatial and nonspatial models; as the spatial scales shrink, the third-moment approximation must fail at some point. We expect moment equations to be most useful, performing significantly better than nonspatial models, at intermediate spatial scales.

Figure 3 shows the equilibrium values of n and $\bar{c}$ for a range of spatial scales as predicted by stochastic simulations (parameters except for λ as in Fig. 2), numerical solutions of the moment equations, and a small-λ (large spatial scale) approximation discussed in the next section. For values of λ in the range 0.1–1.0 (neighborhood size from 20 to 2, or 400–40 neighbors for these parameters), the moment equations match the spatial simulation results closely, but the simulation results also overlap with the nonspatial model. For $\lambda = 1$–5 (neighborhood of 1 to 0.2, or 40–8 neighbors), the mean drops and the average covariance rises (as clusters develop, intensifying local competition); in this range, the moment equations track the simulation results. Finally, for extremely short spatial scales ($\lambda > 5$), the second-order approximation—and the analytically useful, but even more restricted small-λ approximation—starts to break down. It is highly encouraging that the moment equations work well to predict significant amounts of clustering (variance-to-mean ratios of 2 to 3 (adding 1 to $\bar{c}/n^*$ to include Poisson variation), leading to depressions in the mean of 10–15%) in an ecologically relevant range of spatial scales, with moderate neighborhood sizes ($\approx$8–40 neighbors).

Moving to a more detailed look at the equilibrium spatial structure of the moment equations and the simulations, Fig. 4 shows the time-averaged equilibrium covariance for two sets of parameters. Both sets of parameters represent species with a carrying capacity of

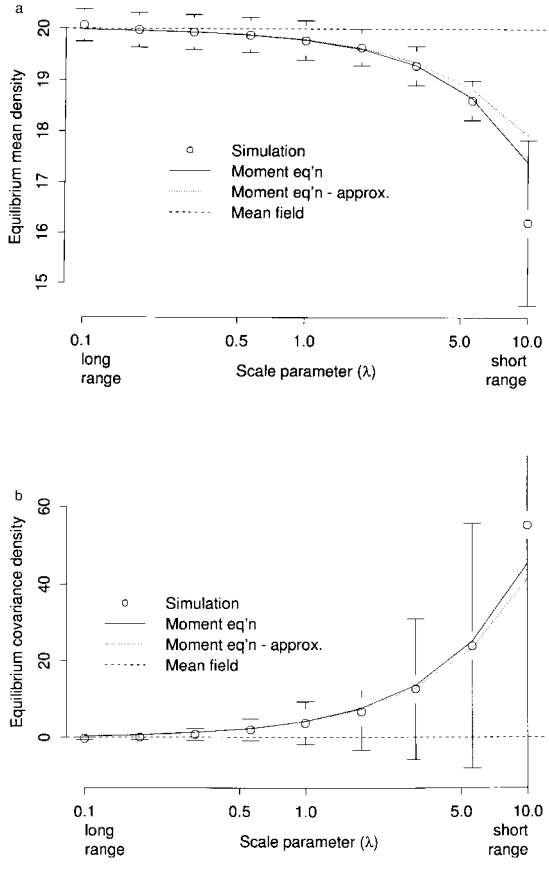

FIG. 3. Simulation and moment equation results, varying spatial scales. Using Laplacian kernels and parameters $f = 0.8$, $\mu = 0.4$, $\alpha = 0.02$, $\lambda_d = \lambda_u$ (always equal to each other) ranging from 0.1 to 10. For Laplacian kernels, the standard deviation of the kernels (scale) is equal to $1/\lambda$, so the figure shows dispersal and competition moving from long-range to short-range from left to right.

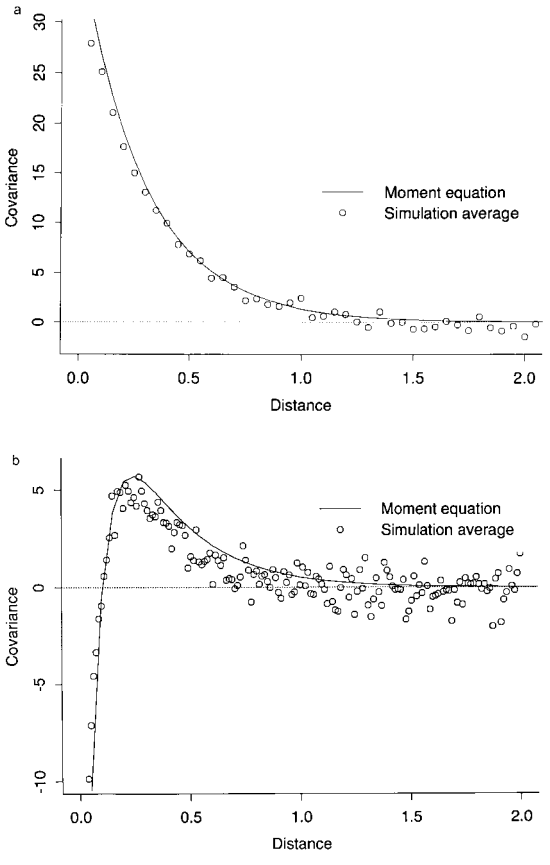

FIG. 4. Equilibrium covariances vs lag for stochastic simulation and numerical solutions of the IPDE system. *Dots* represent the mean (time-average) covariance at a particular lag over a long run of stochastic fluctuations around the equilibrium; *solid line* shows the prediction of the moment equations. (The nonspatial model would predict zero covariance.) (a) Late-successional species, clustered distribution (average over 1000 time steps). Parameters (as in Fig. 2): $f = 0.8$, $\mu = 0.4$, $\alpha = 0.02$, $\lambda_d = \lambda_u = 5.0$. (b) Early-successional species, regular distribution (average over 200 time steps). Parameters are $f = 3.2$, $\mu = 0.4$, $\alpha = 0.14$, $\lambda_d = 5.0$, $\lambda_u = 10.0$.

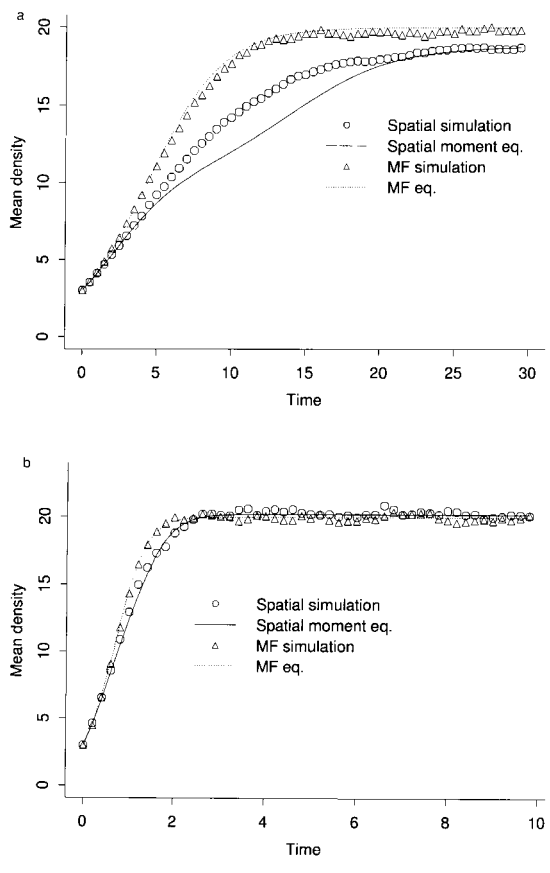

FIG. 5. Time-dependent mean densities for stochastic simulation and numerical solutions of the IPDE system. Means of 30 simulations, each with (spatial) length 100 and starting condition $n(0) = 3.0$, $c(r) = 0$ for all r. (a) Late-successional species. Parameters as in Fig. 4a. (b) Early-successional species, Parameters as in Fig. 4b.

20 in the (nonspatial) logistic model. One model species is a shade-tolerant or late-successional type, with low fecundity but a low density-dependent death rate parameter, meaning it is slow-growing but relatively unaffected by competition. In this species locally dispersed offspring survive to create clusters, leading to clustering (positive average covariance, Fig. 4a). The other species is a shade-intolerant, early-successional type with high fecundity and density-dependent death; it tolerates competition poorly and self-thins until it reaches a stable regular distribution (negative average covariance, Fig. 4b). The moment equations approximate the equilibrium covariances extremely well.

Finally, Fig. 5 shows the growth trajectories of the mean density for the late- and early-succesional model species, again comparing stochastic simulations with the predictions of the moment equations.

As in Fig. 2, the time evolution of mean density for both species appears logistic, with some modification from the effects of spatial structure. The moment equation approximation is slightly worse in the middle part of the growth curve; there are transient higher moments in the spatial patterns of the simulations which cannot be predicted by the moment equations.

It is also possible to derive an expression for the initial growth of the mean and covariance when the system starts from low-density and near-random conditions (density and covariance both $\ll 1$) by linearizing around the zero equilibrium. Here, however, we run into a potential weakness of the second-order approximation. For this system, in addition to the stable internal equilibrium $\{n^*, c^*(r)\}$ that we have have discussed up to now, there is a saddle point at a small value of n and an intermediate

value of $\bar{c}$ and an equilibrium at $\{c(r) \to \infty, n \to -\infty\}$. The upshot is that, when starting at small values of n and c, the covariance can overshoot and reach a point where it grows without bound, driving n down and making the system crash. We emphasize that this is a mathematical problem with the second-order approximation, not an ecological phenomenon; in the full stochastic system, higher moments always slow the growth of the covariance and prevent the crash.

3. EQUILIBRIUM ANALYSIS

In this section we calculate the equilibrium density and spatial structure for the spatial density-dependent mortality model and explore the determinants of equilibrium spatial pattern. The analysis reflects the basic idea that there are three forces operating: random thinning by density-independent mortality, local density-dependent mortality (which reduces clustering), and local dispersal (which increases clustering). Most of the mathematical detail of this analysis is given in Appendix D; this section focuses on the results rather than the methods.

By using the equations for the mean and covariance (Eqs. (6) and (7)) and specializing to the case of Laplacian kernels (Appendix D), we can derive an expression for the equilibrium covariance which is a sum of two Laplacians with scale parameters $\lambda_d\phi_+$ and $\lambda_d\phi_-$, where ϕ_+ and ϕ_- are functions of the parameters:

$$c^*(r) = n^*(g_+ \mathscr{L}(\lambda_d\phi_+) + g_- \mathscr{L}(\lambda_d\phi_-)) = \frac{\lambda_d n^*}{2}(g_+\phi_+ e^{-\lambda_d\phi_+|r|} + g_-\phi_- e^{-\lambda_d\phi_-|r|}). \quad (9)$$

Calculating $\bar{c}^*$ from $c^*(r)$ by integrating $\mathscr{L}(\lambda_u, r)c^*(r)$ (defining ε as λ_u/λ_d),

$$\bar{c}^* = \frac{\lambda_u n^*}{2}\left(\frac{g_+\phi_+}{\varepsilon+\phi_+} + \frac{g_-\phi_-}{\varepsilon+\phi_-}\right). \quad (10)$$

At equilibrium,

$$n^* = \frac{f-\mu'}{\alpha} - \frac{\bar{c}^*}{n^*}; \quad (11)$$

Equations (10) and (11) form a system that can in general only be solved numerically (because $\phi_\pm$ and $g_\pm$ depend on n^*). Fig. 6 shows contours of $-\bar{c}^*/(n^*)^2$ for varying values of ε and μ/f.

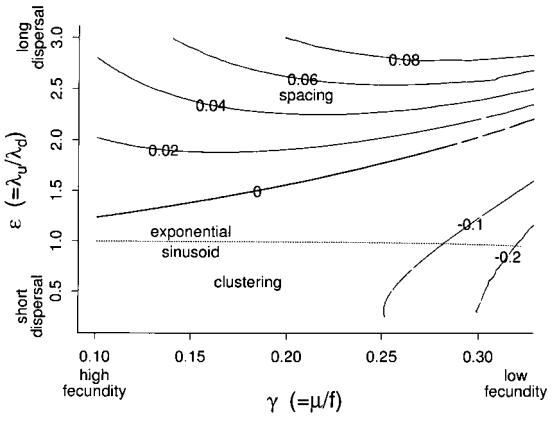

FIG. 6. Effects of spatial structure as a function of population parameters; change in mean density as a proportion of the non-spatial carrying capacity ($-\bar{c}^*/(n^*)^2$). Horizontal axis shows mortality/fecundity ratio ($\mu = 0.4$, f varies); vertical axis shows ε, the ratio of competitive to dispersal scales. Other parameters are $\alpha = 0.14$, $\lambda_d = 5.0$. Bold line shows the zero contour (zero net effect of spatial structure); the dotted line shows the boundary between exponential and sinusoidal covariances. (Note different contour spacings above and below zero.)

We can get farther in the case where λ_d and λ_u are both small (corresponding to long-range dispersal and competition scales), and we can drop higher order terms in λ_d or λ_u. In particular, we will say that $n^* \approx (f-\mu)/\alpha$ in (10). In the final expression the fecundity and mortality parameters only occur in the combination μ/f, the reciprocal of lifetime fecundity in the absence of competition, which we define as γ. We get (Appendix D):

$$\phi_\pm^2 = \varepsilon^2\left(\frac{\gamma}{2} - 1\right) \pm \frac{\varepsilon}{2}\sqrt{\varepsilon^2(2-\gamma)^2 - 4(1-\gamma)} \quad (12)$$

$$g_\pm = \mp\frac{1}{\phi_\pm^2} \cdot \frac{(\phi_\pm^2 - \varepsilon^2)(\phi_\pm^2 - 1)}{\phi_+^2 - \phi_-^2}. \quad (13)$$

If the quantity under the square root in (12) is negative (when $\varepsilon^2 < 4(1-\gamma)/(2-\gamma)^2$), then the coefficients of the two Laplacians ($\phi_\pm$) are complex conjugates of each other and the equilibrium shape of the covariance is a damped sinusoid. Because fecundity must be greater than density-independent mortality in order for a plant population to establish itself at all, γ ranges from 0 to 1. As γ goes from 0 to 1, the threshold value of ε below which the covariance is sinusoidal goes monotonically from 1 to 0. When the covariance is sinusoidal, we have

$$c^*(r) = \frac{\lambda}{2} e^{-\lambda\phi_r|r|}(g_c \cos(\lambda\phi_i|r|) + g_s \sin(\lambda\phi_i|r|)) \quad (14)$$

$$g_c = 2(\phi_r g_r - \phi_i g_i) \quad (15)$$

$$g_s = 2(\phi_r g_i + \phi_i g_r), \quad (16)$$

where g_r and g_i are the real and imaginary parts of g_+ (g_+ and g_- are complex conjugates as well as ϕ_+ and ϕ_-) and ϕ_r and ϕ_i are the real and imaginary parts of ϕ_+.

These expressions are still too complicated. One simpler case is when dispersal becomes nearly global, and only mortality affects the spatial pattern of individuals ($\lambda_d \to 0$). Then

$$c^* = n^*(\gamma - 1) \cdot \mathscr{L}(\lambda_u \phi) \tag{17}$$

$$\phi = \sqrt{\frac{1}{1-\gamma}}. \tag{18}$$

In this case the covariance is always exponential and $\bar{c}^*$ is always negative for ecologically feasible parameters, as would be expected when the only source of clustering (local dispersal) has been eliminated. (When competition becomes global ($\lambda_u \to 0$), the moment approximation breaks down: in the moment equations, clustering becomes infinite because there is no brake on it, but it does not affect the mean density because the "local" and global mean density become the same.)

Another special case is when the competition and dispersal scales are equal ($\lambda_d = \lambda_u, \varepsilon = 1$). Then (still assuming $\lambda_u, \lambda_d \ll 1$)

$$c^*(r) = n^* \frac{1}{(1/\gamma) - 1} \cdot \mathscr{L}(\lambda\phi) \tag{19}$$

$$\phi = \sqrt{1-\gamma}. \tag{20}$$

In this case the covariance is again exponential, but equilibrium spatial covariance is always positive.

In general, we can write the equilibrium covariance as a sum of two Laplacians, with different scale parameters and different coefficients. Given an observed equilibrium covariance we could recover the values of the scale parameters and coefficients by fitting a sum of two exponentials. Along with the mean density, this would give us five pieces of information; we might think therefore that we could recover all five parameters (dispersal scale λ_d, competition scale λ_u, fecundity f, density-independent mortality μ, density-dependent mortality α) of the original model from the equilibrium mean and covariance (we assume λ_d and λ_u are small so that the equilibrium mean density is close to the nonspatial value).

However, interdependence between the parameters leads to only four degrees of freedom. With a little algebra we can recover all the spatial information (competition and dispersal scales) and two pieces of information about life history and competition (e.g., net lifetime fecundity in a noncompetitive environment (r/μ) and the ratio of density-independent to density-dependent mortality (μ/α), but we cannot get any information about the time scales of the dynamics (f, μ, or r) from equilibrium patterns alone. To get this information we would have to perturb the equilibrium or observe an invasion. These results match the simpler case of the classical logistic equation, where the equilibrium mean tells us about equilibrium properties (carrying capacity, K) but not the dynamics (r).

4. EXTENSIONS OF THE MODEL

4.1. Two Dimensions

Although the derivations of the mean and covariance equations themselves are valid for general choices of competition and dispersal kernels in any number of dimensions, all of the equilibrium results presented in the previous section are for one-dimensional systems with Laplacian kernels. Conveniently, all of the results on equilibrium solutions are easy to extend to more than one dimension, provided that the multidimensional models use particular kernels which are analogous to the Laplacian kernels used in one dimension. (We will discuss the two-dimensional case here; the three-dimensional case is equally straightforward but harder to make relevant to ecological questions.)

In particular, the equilibrium solutions (Appendix D) make use of some special properties of the Fourier-transformed Laplacian kernel $\tilde{\mathscr{L}}(q_r)$, which is $\lambda^2/(\lambda^2 + q_r^2)$. If we can find multidimensional kernels with the same Fourier transform (with $q_r^2 = q_x^2 + q_y^2$ or $q_x^2 + q_y^2 + q_z^2$), then all of the results derived above follow immediately for the multidimensional case. For two dimensions, the inverse Fourier transform of $\lambda^2/(\lambda^2 + q_r^2)$ is the modified Bessel function of order 0. Although its integral is well-behaved, this kernel has a singularity at $r = 0$, which means we must explicitly set self-competition ($U(0)$) to zero, rather than incorporating self-competition into the density-independent mortality term. Note that this distribution is biologically realistic as well as analytically convenient: it represents the distribution obtained when individuals disperse randomly in two dimensions from their starting point and settle (stop moving) with a constant rate over time, and has been used as a dispersal curve in biological models before (van den Bosch *et al.*, 1988).

The equilibrium value of $c(r)$ given above (Eq. (9)) remains the same in two dimensions, with the exception that the Laplacian kernel $\mathscr{L}(\lambda, r) = \lambda/2 \exp(-\lambda r)$ is

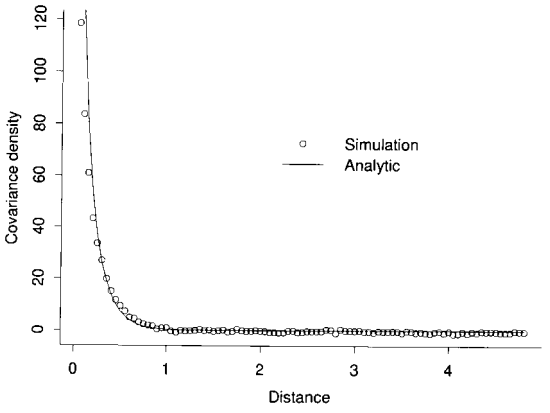

FIG. 7. Average covariance density vs distance for a two-dimensional system with the same parameters as in Figs. 2 and 5, except for the dispersal and competition kernels which are Bessel functions with scale parameter $\lambda_d = \lambda_u = 3\pi$ giving an average interaction distance $= 1/3$ (Fig. 1 shows a snapshot of this system). *Points* show the average covariance over 350 time steps at equilibrium; *lines* show the equilibrium covariance predicted from the moment equations.

replaced by the Bessel function. However, the equilibrium value of $\bar{c}^*$ does change in two dimensions. In one dimension, the relevant calculation is that

$$\int_{-\infty}^{\infty} U(r)\, c(r)\, dr \propto \int_{-\infty}^{\infty} \mathscr{L}(\lambda\varepsilon, r)\, \mathscr{L}(\lambda\phi, r)\, dr = \frac{\lambda\varepsilon\phi}{2(\varepsilon+\phi)}; \tag{21}$$

in two dimensions

$$\int_0^{2\pi} \int_{-\infty}^{\infty} U(r)\, c(r)(r dr)\, d\theta = \frac{\lambda^2\phi^2\varepsilon^2 \log(\phi/\varepsilon)}{2\pi(\phi^2-\varepsilon^2)}. \tag{22}$$

Using (22) for $\bar{c}^*$ instead of (10), we can follow the same strategies used in Section 3—numerical solution of the system of equations for $\bar{c}^*$ and n^*, or a small-λ, long-range approximation that makes the system analytically solvable.

For example, Fig. 7 shows the average covariance density (over several hundred time steps at equilibrium) and the predicted equilibrium covariance density for the moment equation system for the simulation illustrated in Fig. 1.

4.2. Other Extensions

There are many extensions to the basic model presented here that incorporate ecologically interesting mechanisms. At the simplest level, we can explore the effects of other competitive interactions such as density-dependent fecundity or density-dependent establishment, where the fecundity of an adult or the establishment probability of a newly dispersed seed decreases with increasing local density. In the limit of the classical logistic model, all of these competitive mechanisms are the same, but in the spatial stochastic model they can differ in interesting ways.

Perhaps the most important ecological piece missing from the current model is the possibility of nonlinear competitive interactions, for example a hyperbolic or exponential decay of fecundity with local crowding (Pacala, 1986). Nonlinearity ruins the simple averaging process used in our derivations (because $E[f(N)]$ no longer equals $f(E[N])$), but preliminary work suggests that expanding around the conditional mean, $E[N(y) \mid N(x)]$, will make a good approximation.

Other straightforward extensions (just mentioned in passing here) which will vastly extend the applicability of these models to real systems are the incorporation of size-structured and asymmetric competition; environmental heterogeneity (characterized by its spatial covariance); mechanistic plant-resource interactions, including dynamically (and spatially) varying resource levels; and multiple-species interactions. Deriving moment equations incorporating each of these extensions is easy but full analyses of the dynamics and equilibria of each phenomenon, not to mention their interactions, will take time and effort.

5. DISCUSSION AND CONCLUSIONS

We have shown that second-order moment equations can capture the essential properties of dynamical spatial pattern formation. The approximation that third spatial moments are negligible is good enough to predict the formation of strong spatial patterns with significant ecological effects, increasing local neighborhood densities and decreasing overall mean densities by $\approx 30\%$ (Figs. 1 and 7). One caveat is that endogenous pattern formation may not be relevant to natural single-species plant populations, because lifetime fecundity in the absence of competition ($1/\gamma$) is usually in the hundreds or thousands (Harper and White, 1974), which leads to regular spacing or to weak clustering (Fig. 6). However, preliminary work with multispecies models suggests that spatial pattern formation and in particular spatial segregation can have major effects on interspecific interactions.

Moment equations model spatial dynamics in ways that match our intuitions about clustering and competi-

tion; they also preserve continuous space, stochasticity, and analytical tractability in a way that few other approaches to modeling spatial interactions can match. In addition to their heuristic and theoretical value, they can be computationally useful in summarizing the typical behavior of a highly variable stochastic simulation model across an ensemble. For example, producing Fig. 6, summarizing the behavior of an individual-based stochastic simulation throughout a two-dimensional phase space, would be tedious to do by brute force.

Despite its strengths, the moment equation approach shares some of the limitations of continuous-density models. It assumes a homogeneous environment (although we are developing ways of incorporating environmental variability in the equations), and like the continuous-density models it sometimes demands fairly heavy analytical machinery.

The other potential weakness of the moment equation approach is that it only applies when third spatial moments are sufficiently small. The ecologically sensible cases presented here have small enough third moments; under what other circumstances will this approximation be valid? The results of the simulations suggest that the approximation breaks down for small numbers of neighbors; this phenomenon is probably general. A few attempts at deriving approximations for one-dimensional nearest-neighbor models such as the contact process have given very poor results, misestimating the threshold for persistence by a large amount. As suggested in Section 2.3, however, the ecological realities of competitive and other interactions are more likely to be "many neighbors" than "nearest-neighbor." We are still not sure what kinds of spatial patterns will have large third moments. The third spatial moment is related to the variance in neighborhood density—spatial patterns with more variable neighborhoods (within the constraints of a given mean density and covariance pattern) will have higher third moments. Heuristic arguments suggest that patterns with sharp boundaries (such as "checkerboard" patterns) will also tend to have large higher-order spatial moments.

Our theoretical approach relies on averages across infinite ensembles of realizations of a population-dynamic system. In experimental and particularly in field observations, it will be difficult to obtain large numbers of realizations of the same system. There are two ways around this problem: first, the same conditions may recur in a system (for example, in repeated epidemic waves or invasions) and be treatable as separate realizations. Second, if the system is fluctuating in some consistent manner, either around an equilibrium or in a disturbance regime that stays constant over appropriate scales, one can use space or time as a proxy for different realizations, sampling the system at places or times that are far enough apart to be considered independent. Formally, this is attributing an *ergodic* property to the system, and it should work well in practice if a large enough area can be sampled: the simulation equilibrium covariances presented in this paper (Figs. 4 and 7) show time averages of (presumably) ergodic fluctuations around the equilibrium covariance.

We can actually estimate the size of the third moments in a particular spatial point pattern. A standard estimator of spatial covariance in point process theory is the "K function" (Ripley, 1981; Diggle, 1983); $K(r)$ is proportional to the expected number of neighbors within a distance r of an arbitrary plant. By analogy, we can define $K_3(r)$ as the number of pairs of neighbors within a distance r of an arbitrary plant, which is related to the *variance* of the number of neighbors within a neighborhood radius r. This summary measurement provides a way to estimate the integrated third moment and hence an indicator of how much error is introduced in the model by ignoring the third moment term.

The moment equation approach developed in this paper has much wider application than the example of plant competition presented here. Any simple pairwise interaction that takes place in space can be modeled in the same way, taking expectations to get evolution equations for the mean densities and the spatial covariances of all actors. Two obvious classes of potential applications are predator–prey models and host–parasite or epidemic models. Other kinds of models will continue to be appropriate for ecological systems with strongly nonhomogeneous spatial structure and complicated rules, but moment equations could provide insight into a large variety of basic ecological systems.

APPENDIX A: DERIVATION OF THE MEAN EQUATION

There are two possible routes to take in deriving the ensemble equations, two alternate ways of dealing with the problem of correctly averaging a point density process with infinite Dirac δ functions across an infinite number of realizations to come up with smooth, bounded densities and covariance densities. One route is more formal, the other more heuristic, although both can be made precise. Here we give a brief description of the formal approach, but concentrate on the heuristic argument.

The formal way of deriving the equations defines an auxiliary variable which is the stochastic cumulative density function, in one dimension $N(x, \Gamma) = \int_{-\infty}^{x} n(y)\, dy$: this quantity is the number of individuals to the left of x in a stochastic realization denoted by Γ. The cumulative density function is a sum of step functions rather than the Dirac δ functions of the density itself, and so it is straightforward to average across realizations by integrating with respect to Γ. However, using the cumulative density function adds enough complexity that we prefer the heuristic derivation.

The heuristic derivation starts with a system on a lattice, rather than with a point process, derives the expected change in mean density of lattice cells, then takes the limit as the lattice size shrinks to zero. The lattice has no real place in the definition of the system; it is just a useful device for reaching the ensemble average without dealing with Dirac δ functions more than necessary.

We start by taking the definition of the continuous-time stochastic process in a box of size ω, in this case Eq. (3) above, and calculating the expected change in the state of a box at location x between times t and $t + \Delta t$, conditional on the entire state of the system. $N(x, t)$ denotes the number of individuals within a box of size ω located at x at time t, and $\bar{x}$ denotes an expectation with respect to all possible changes in the system.

$$\begin{aligned}\overline{\Delta N(x)} &= [\,(+1 \cdot \text{birth rate} - 1 \cdot \text{death rate}]\,\Delta t \\ &= \Bigg[f \sum_y D(y-x)\, N(y)\, \omega - N(x) \\ &\quad \times \left(\mu + \alpha \sum_y U(y-x)\, N(y) \right) \Bigg]\, \Delta t. \qquad \text{(A1)}\end{aligned}$$

The sums are over all space and Δt and ω are both $\ll 1$, small enough so that the probability of two events happening within Δt or of a box containing more than one plant is negligible: $N(x) \in \{0, 1\}$. Throughout this derivation, x denotes a focal location; y denotes a particular location from which new plants could colonize x; and z denotes the location of a competitor of a plant at y.

Now we take expectations again, this time over an infinite *ensemble* of possible states $\{N(x)\}$ of the system. We do not know the probability distribution of states of the system, but we know that the expectation exists (because $N(x) \in \{0, 1\}$) and we take the same expectation on both sides of the equation.

$$\begin{aligned}\frac{\langle \overline{\Delta N(x)} \rangle}{\Delta t} &= f \sum_y D(y-x)\, \omega \langle N(y) \rangle \\ &\quad - \left\langle N(x) \left(\mu + \alpha \sum_y U(y-x)\, N(y) \right) \right\rangle \qquad \text{(A2)}\end{aligned}$$

Since we choose ω such that $N(x)$ is never greater than one, $\langle N(x) \rangle \in [0, 1]$ and can be interpreted as the probability of finding an individual in a box of width ω located at x.

Note that the density of plants per box, $\langle N \rangle$, is independent of spatial position; when the covariance appears in the derivation, it will depend only on lag (distance between two points), not on the position of either point. Since the rates of the stochastic processes in this system are either position-independent (death depends only on $N(x)$, not on x) or depend only on relative position (competition and dispersal are functions of $N(x)$, $N(y)$, and $|x - y|$), only the initial conditions could provide an absolute origin. Homogeneous initial conditions (such as a Poisson distribution), and non-homogeneous initial conditions with a random origin in each realization both produce ensembles where the mean density is the same everywhere in space. In physics jargon, this property is called "translation invariance;" in statistics, "spatial stationarity." Translation invariance does not necessarily mean that a particular realization is homogeneous; it just means that any given pattern can occur anywhere in space, so that averaging over all possible realizations gives a homogeneous probability density over space.

Using translation invariance, $N \equiv \langle N(0) \rangle = \langle N(x) \rangle$ is the expected average density (we can set $x = 0$ without loss of generality):

$$\frac{\langle \overline{\Delta N} \rangle}{\Delta t} = (f - \mu)\, N - \alpha \sum_y U(y) \langle N(0)\, N(y) \rangle. \qquad \text{(A3)}$$

This expression has been simplified by taking terms out of the expectation wherever possible: in particular, since N is independent of y and because D is a probability distribution ($\sum D(y)\omega \approx 1$), $\sum_y (D(y) N(0))\omega = fN$.

(We do not actually need to assume translation invariance (Lewis and Pacala [see p. 18] (1997) analyze a problem with spatially dependent sources), but it simplifies the analysis considerably.)

The next step in the derivation is to expand the $\langle N(0)\, N(y) \rangle$ terms. This term represents the expected joint density of points 0 and y, which because of translation invariance depends only on y, the distance between focal individuals. We define the expansion of $\langle N(0)\, N(y) \rangle$ as

$$\langle N(0) N(y) \rangle = N^2 + \text{Cov}(y), \qquad \text{(A4)}$$

the expected joint density in the independent case plus the *spatial covariance* between densities at two locations a distance y apart.

The case $y = 0$ is special: we define the variance Var as $\langle N(0)^2 - N^2 \rangle$. Var is formally equivalent to Cov(0), but it scales differently from the rest of the covariance and is most simply incorporated as a separate term. Later in the derivation we will substitute in $\sigma^2 \equiv \lim_{\omega \to 0} \mathrm{Var}/\omega = n$. (*Proof.* Since we have defined the lattice size ω so that $N(x) \in \{0, 1\}$, $N(x)$ and $N(x)^2$ are always equal, so $\mathrm{Var} = \langle N(x) \rangle - N^2$. Dividing through by ω and using the definitions of σ^2 and n, we get $\sigma^2 = n - n \cdot N$. Taking the limit as $\omega \to 0$, N goes to zero while n stays finite, so $\sigma^2 = n$ as claimed.) The variance term can be incorporated either by taking the $x = y$ (zero lag) term out of summations before scaling, or equivalently by recognizing that the covariance actually has a Dirac δ function at lag zero that integrates to n ($\int_{0-}^{0+} c(r)\, dr = n$).

Using (A4), and rearranging,

$$\frac{\langle \overline{\Delta N} \rangle}{\Delta t} = \left(f - \mu - \alpha \frac{N}{\omega} \right) N - \alpha U(0)\, \mathrm{Var} - f \sum_{y \neq 0} D(y)\, \mathrm{Cov}(y)\, \omega - \alpha \sum_{y \neq 0} U(y)\, \mathrm{Cov}(y). \tag{A5}$$

We now divide both sides of the equation by ω and substitute density $n \equiv N/\omega$, variance density $\sigma^2 \equiv \mathrm{Var}/\omega$, and covariance density $c(r) \equiv \mathrm{Cov}(r)/\omega^2$. We define the covariance c so that it excludes the point at zero, which is the variance term, producing:

$$\frac{\overline{\Delta n}}{\Delta t} = (f - \mu - \alpha n)\, n - \alpha U(0)\, \sigma^2 - f \sum_{y \neq 0} D(y)\, c(y)\, \omega^2 - \alpha \sum_{y \neq 0} U(y)\, c(y) \omega. \tag{A6}$$

Now we can scale $\omega \to 0, \Delta t \to 0$ (moving to continuous time and space) to get

$$\frac{dn}{dt} = (f - \mu - \alpha n)\, n - \alpha U(0)\, \sigma^2 - \alpha \int_{y \in \Omega} U(y)\, c(y)\, dy. \tag{A7}$$

We substitute $\sigma^2 = n$, as proved above, and set $\mu' \equiv \mu + \alpha U(0)$ to account for unavoidable self-competition (in practice, any measurement of baseline mortality will already include this correction) to obtain (finally) the desired equation for the change over time in average density as a function of density and covariance (Eq. (6)).

APPENDIX B: DERIVING THE COVARIANCE EQUATION

Deriving the equation for the change in covariance over time involves the same basic steps as the mean equation (Appendix A), but more complicated algebra. We use the same procedure of taking expectations and scaling, but this time we are interested in the quantity

$$\begin{aligned} \langle \overline{\Delta \mathrm{Cov}(y - x)} \rangle &= \langle \overline{\Delta (N(x) \cdot N(y) - N^2)} \rangle \\ &= \langle N(x)\, \overline{\Delta N(y)} \rangle + \langle N(y)\, \overline{\Delta N(x)} \rangle \\ &\quad - 2N\, \overline{\Delta N}. \end{aligned} \tag{B1}$$

The second equation follows by assuming that Δt is small enough so that $\Delta(N(x) \cdot N(y))$, the probability per unit time of events happening at both x and y, is negligible (we assume throughout this section that $x \neq y$, since we already know that the covariance at zero lag is equal to the mean).

Using the translation invariance property to say that we can exchange x and y at will:

$$\langle \overline{\Delta \mathrm{Cov}(y - x)} \rangle = 2 \langle N(x)\, \overline{\Delta N(y)} \rangle - 2N \langle \overline{\Delta N} \rangle. \tag{B2}$$

We find $\langle N(x)\, \overline{\Delta N(y)} \rangle$ by the same methods used in Appendix A, taking the expression for $\overline{\Delta N(y)}$ from (A1), multiplying by $N(x)$, and taking expectations across the ensemble:

$$\begin{aligned} &\langle N(x)\, \overline{\Delta N(y)} \rangle / \Delta t \\ &\quad = -\mu \langle N(x) \cdot N(y) \rangle \\ &\qquad + f \sum_z D(z - y)\, \omega \langle N(x) \cdot N(z) \rangle \\ &\qquad - \alpha \sum_z U(z - y) \langle N(x) \cdot N(y) \cdot N(z) \rangle. \end{aligned} \tag{B3}$$

It helps to keep track of the meanings of the spatial positions x, y, and z. In Appendix A x was a focal position; y was a position that might contain a plant dispersing seeds to point x; and z was a potential competitor of y. Here both x and y are focal positions,

and z is the location of a disperser to x (in the second term of (B3)) or of a competitor of a plant at x (in the third term of (B3)).

In order to decompose $\langle N(x) \cdot N(y) \cdot N(z) \rangle$, we have to define the *third central spatial moment* $M_3(x, y, z)$, analogous to the covariance:

$$\begin{aligned} &M_3(x, y, z) \\ &\quad = \langle (N(x) - \langle N \rangle) \cdot (N(y) - \langle N \rangle) \cdot (N(z) - \langle N \rangle) \rangle \\ &\quad = \langle N(x) \cdot N(y) \cdot N(z) \rangle - N(\mathrm{Cov}(x-y) \\ &\qquad + \mathrm{Cov}(x-z) + \mathrm{Cov}(y-z)) - N^3 \end{aligned} \tag{B4}$$

(provided $x \neq y$, $y \neq z$, and $z \neq y$). With this definition and the definition of the covariance ($\mathrm{Cov}(x-y) = \langle N(x) \cdot N(y) \rangle - N^2$), we get:

$$\begin{aligned} &\langle N(x)\, \overline{\Delta N(y)} \rangle / \Delta t \\ &\quad = \left(f - \mu - \alpha \frac{N}{\omega} \right) N^2 - \mu\, \mathrm{Cov}(x-y) \\ &\qquad + f \sum_z D(y-z)\, \omega\, \mathrm{Cov}(x-z) - \alpha N \sum_z U(z-y) \\ &\qquad \times (\mathrm{Cov}(x-y) + \mathrm{Cov}(y-z) + \mathrm{Cov}(x-z)) \\ &\qquad - \alpha \sum_z U(z-y)\, M_3(x, y, z). \end{aligned} \tag{B5}$$

As in the derivation of the mean, we have used the fact that D and U are defined as probability density functions (i.e., $\sum_{r \in \Omega} D(r)\omega \equiv 1$) when pulling constant terms out of the sums.

At most points $M_3(x, y, z) \propto \omega^3$, just as $\mathrm{Cov} \propto \omega^2$ and $N \propto \omega$. However, as with the covariance, if any two of the three points defining M_3 coincide ($x = y$, $x = z$, or $y = z$), then $M_3 \propto \omega^2$ instead (because $N(x)^2 = N(x)$ if $N(x) \in \{0, 1\}$: for example, $\langle N(x)^2\, N(y) \rangle = \langle N(x)\, N(y) \rangle = N^2 + \mathrm{Cov}(x-y)$). Treating all of these singular points separately (defining M'_3 as excluding points where any two of x, y, and z coincide) gives

$$\begin{aligned} &\langle N(x) \cdot N(y) \cdot N(z) \rangle \\ &\quad = [\, N(\mathrm{Cov}(x-y) + \mathrm{Cov}(x-z) + \mathrm{Cov}(y-z)) \\ &\qquad + N^3 + M'_3(x, y, z)\,](1 - \delta_{xz})(1 - \delta_{yz})(1 - \delta_{xy}) \\ &\qquad + \delta_{xz}(1 - \delta_{xy})(N^2 + \mathrm{Cov}(x-y)) \\ &\qquad + \delta_{yz}(1 - \delta_{xy})(N^2 + \mathrm{Cov}(x-y)) \\ &\qquad + \delta_{xy}(1 - \delta_{yz})(N^2 + \mathrm{Cov}(y-z)) + \delta_{xyz} N \end{aligned} \tag{B6}$$

(the last term applies when $x = y = z$). The δ_{xy} and δ_{xyz} terms drop out in the equations below because we are not considering the variance ($x = y$) term. As with the variance (Appendix A), taking the singular points out in this way is formally equivalent to saying that there are Dirac δ functions in the third moment density, m_3, which we define as M'_3/ω^3 (making it analogous to c).

Now we discard m_3, assuming it is much smaller than all other terms, which is the single approximation involved in the derivation of the moment equations.

Using (B6), dividing both sides of (B5) by ω^2, substituting n and c as in Appendix A, and letting $\omega \to 0$:

$$\begin{aligned} &\langle n(x)\, \overline{\Delta n(y)} \rangle / \Delta t \\ &\quad = -\mu c(x-y) + f \left(\int D(y-z)\, c(x-z)\, dz + D(x-y)\, n \right) \\ &\qquad - \alpha n \left(\int U(x-z)\, c(y-z)\, dz + U(x-y)\, n + c(x-y) \right) \\ &\qquad + \Bigg[(f - \mu - \alpha n)\, n^2 - \alpha n \\ &\qquad \times \left(\int U(x-z)\, c(x-z)\, dz + U(0)\, n \right) \Bigg]^{\dagger} \\ &\qquad + [\, -\alpha U(0)\, c(x-y)\,]^{\ddagger} \\ &\qquad + [\, -\alpha U(x-y)\, c(x-y)\,]^{\S} \end{aligned} \tag{B7}$$

(the integrals have also been simplified wherever possible).

We can simplify (B7) in a number of ways. We have been considering just $\langle N(x)\, \overline{\Delta N(y)} \rangle$: the full covariance is $2\langle N(x)\, \overline{\Delta N(y)} \rangle - 2N\Delta N$. When we subtract off the $N\Delta N$ term, the terms above marked with (†) cancel. The term marked with (‡) is a self-competition term (it includes $U(0)$), and we can incorporate it into the first term above by setting $\mu' = \mu + \alpha U(0)$ as in Appendix A. Finally, the term marked with (§) remains, but it is a third-moment singular term that we will drop when we analyze the equilibrium of the system.

$$\begin{aligned} &\Delta c(x-y)/\Delta t \\ &\quad = 2 \Bigg[-\mu' c(x-y) \\ &\qquad + f \left(\int D(x-z)\, c(y-z)\, dz + D(x-y) n \right) \\ &\qquad - \alpha n \left(\int U(x-z)\, c(y-z)\, dz + U(x-y)\, n + c(x-y) \right) \\ &\qquad + [\, -\alpha U(x-y)\, c(x-y)\,]^{\S} \Bigg]. \end{aligned} \tag{B8}$$

Finally, we use translation invariance to set $x \equiv 0$, let $\Delta t \to 0$, and use the convolution notation (Eq. (8)):

$$\frac{\partial c(y)}{\partial t} = 2 \times [\, -\mu' c(y) + f((D * c)(y) + D(y)\, n) - \alpha n((U * c)(y) + U(y)\, n + c(y)) - (\alpha U(y)\, c(y))^{\S}]. \quad \text{(B9)}$$

In the equilibrium analysis (Appendix D), we will drop the third-moment singular term (§). We have no formal mathematical justification for dropping this term—in the limit of small λ it will scale as the rest of the terms we keep in the covariance equation, not as the third central moment term that we drop. It will be analytically convenient, however, because all of the other terms in the covariance equation (B9) involve only the covariance (c) or convolutions of the kernels (U and D) with the covariance, which can be easily handled by Fourier transforming the equation (Appendix D). Dropping this term is practically justified because the moment equations still work; all of the results shown in the main text exclude the third moment singular term.

APPENDIX C: DETERMINISTIC ANALOGUE OF THE MOMENT EQUATIONS: STABILITY ANALYSIS

To get the deterministic analogue of the moment equations, simply take Eq. (A1) and scale $N(x)$ to a density $n(x) = N(x)/\omega$ immediately, without taking expectations across an ensemble:

$$\frac{\overline{\Delta n(x)}}{\Delta t} = -\mu n(x) + f \sum_z D(x-z)\, \omega n(z) - \alpha n(x) \sum_z U(x-z)\, n(z)\, \omega. \quad \text{(C1)}$$

In the limit of a large number of individuals each exerting an infinitesimal effect on the others, the stochastic nature of the system vanishes and the density evolves deterministically, so the expectation (denoted by an overbar) on the LHS disappears. In the limit as ω and $\Delta t \to 0$, the result is an integro-differential equation for the behavior of $n(x)$, where $n(x)$ is a spatial density rather than an expected density:

$$\frac{\partial n(x)}{\partial t} = -\mu n(x) + f \int D(x-z)\, n(z)\, dz - \alpha n(x) \int U(x-z)\, n(z)\, dz. \quad \text{(C2)}$$

The mean field (nonspatial) solution is the same as for the stochastic model: $n^* = (f-\mu)/\alpha$. Linearizing around $n(x) = n^* + \eta(x)$ (and using the convolution notation), we get

$$\frac{\partial \eta(x)}{\partial t} = -\mu \eta(x) + f(D * \eta)(x) - \alpha n^*((U * \eta)(x) + \eta(x)). \quad \text{(C3)}$$

Fourier transforms (James, 1995) can be used to find the conditions for which this expression is positive and the system is unstable to perturbations. The Fourier transform is defined as

$$\mathscr{F}(U) = \int_{-\infty}^{\infty} e^{iqx} U(x)\, dx; \quad \text{(C4)}$$

we will also use the notation $\tilde{U}(q) \equiv \mathscr{F}(U(x))$. Fourier transforms express functions of space in terms of spatial frequencies: a sinusoidal pattern transforms to a Dirac δ function at its characteristic frequency. Fourier transforms turn convolutions into products:

$$\mathscr{F}\left(\int a(y-x)\, b(y)\, dy\right) = \mathscr{F}(a * b) = \mathscr{F}(a) \cdot \mathscr{F}(b). \quad \text{(C5)}$$

Fourier transforming (C3) gives:

$$\frac{\partial \tilde{\eta}(q)}{\partial t} = \tilde{\eta}(q)(-\mu + f\tilde{D}(q) - \alpha n^*(1 + \tilde{U}(q))) \quad \text{(C6)}$$

Substituting $n^* = (f-\mu)/\alpha$ and simplifying,

$$\frac{\partial \tilde{\eta}(q)}{\partial t} = \tilde{\eta}(q)(f(\tilde{D}(q) - 1) - (f-\mu)\, \tilde{U}(q)). \quad \text{(C7)}$$

If $f > \mu > 0$, $\tilde{U}(q) > 0$, and $\tilde{D}(q) < 1$ for all q, then the homogeneous state will always be stable against small perturbations at any frequency.

The first condition is true for any system with a positive equilibrium density, and the last two conditions are satisfied by both normal and Laplacian kernels, as well as by the Bessel function (the two-dimensional analogue of the Laplacian); kernels that are sums of Laplacians should also produce the same result.

Thus the homogeneous state is always stable for these kernels. On the other hand, with a competition kernel that is negative for some lags (which would correspond to facilitation), structure could arise in the deterministic system.

The primary differences between the stochastic (Eqs. (A7), (7)) and deterministic (Eq. (C2)) models are the n terms arising from the variance, which allow the generation of a spatial pattern from the homogeneous state.

APPENDIX D: ANALYTIC SOLUTION FOR THE EQUILIBRIUM MEAN AND COVARIANCE

In this appendix we solve for equilibrium solutions of the equations for the mean (Eq. (6)) and the covariance (Eq. (7)). Specifically, we start by finding the equilibrium covariance as a function of n^*, the equilibrium mean; then we can find $\bar{c}$, the average covariance, as a function of n^*, which in turn can be substituted into the n equilibrium equation to give a nonlinear equation for n^* that can be solved numerically. Alternatively, assuming $\lambda \ll 1$ and discarding higher-order terms allows an approximate analytic solution.

All of the analysis presented here depends on special properties of the Laplacian kernel (or its higher-dimensional analogues). We conjecture, however, that the same methods should work, although the analysis would be harder, for kernels which are sums of Laplacians—that is, for any kernel that has a Laplace transform (although some results may be restricted to kernels that are monotonically decreasing in $|x|$).

The easiest way to solve for the equilibrium covariance is to Fourier transform the equilibrium equation (turning convolutions into products (Eq. (C5))), then to substitute in a trial solution for the form of the equilibrium covariance and solve equations for the parameters.

The Fourier-transformed equilibrium covariance equation is (omitting the third-moment singular term)

$$(\mu' - f\tilde{D}(q) + \alpha n(\tilde{U}(q) + 1))\,\tilde{c}(q) - n(f\tilde{D}(q) - \alpha n\tilde{U}(q)) = 0 \qquad \text{(D1)}$$

(We will drop the position indicator q in what follows for notational convenience; $\tilde{D} \equiv \tilde{D}(q)$, $\tilde{U} \equiv \tilde{U}(q)$, etc.) We assume a solution of the $\tilde{c}^*$ of the form

$$\tilde{c}^* = g_+ \tilde{\mathscr{L}}(\lambda\phi_+) + g_- \tilde{\mathscr{L}}(\lambda\phi_-) \qquad \text{(D2)}$$

where $\tilde{\mathscr{L}}$ is the Fourier transform of the Laplacian: $\tilde{\mathscr{L}}(\lambda) \equiv \lambda^2/(\lambda^2 + q^2)$.

Substituting (D2) into (D1), assuming $\tilde{D} = \tilde{\mathscr{L}}(\lambda)$, $\tilde{U} = \tilde{\mathscr{L}}(\lambda\varepsilon)$ (set $\lambda_u = \lambda\varepsilon$), and expanding in partial fractions, using

$$\tilde{\mathscr{L}}(a) \cdot \tilde{\mathscr{L}}(b) = \frac{b^2}{b^2 - a^2}\,\tilde{\mathscr{L}}(a) - \frac{a^2}{b^2 - a^2}\,\tilde{\mathscr{L}}(b), \qquad \text{(D3)}$$

gives an expression of the form

$$C_1\tilde{\mathscr{L}}(\lambda) + C_2\tilde{\mathscr{L}}(\lambda\varepsilon) + C_3\tilde{\mathscr{L}}(\lambda\phi_+) + C_4\tilde{\mathscr{L}}(\lambda\phi_-) = 0. \qquad \text{(D4)}$$

In order for this equation to hold for all values of q (all of the $\tilde{\mathscr{L}}$ are implicitly different functions of q), all of the C_i must be zero. Solving the equations for the C_i gives the values of the four coefficients, $g_\pm$ and $\phi_\pm$, that determine the shape of the equilibrium covariance.

The equations for the $\tilde{\mathscr{L}}(\lambda\phi_+)$ and $\tilde{\mathscr{L}}(\lambda\phi_-)$ coefficients (which are the same up to a change in subscripts) give a quadratic equation for $\phi_\pm^2$:

$$(\mu + \alpha n)\phi_\pm^4 + (f - (\mu + \alpha n)(\varepsilon^2 + 1) - \alpha n\varepsilon^2)\phi_\pm^2 - (f - \mu - 2\alpha n)\,\varepsilon^2 = 0. \qquad \text{(D5)}$$

We can solve for $\phi_\pm$, but the solution is rather complicated. However, if we require $\lambda \ll 1$ (and therefore $n^* \approx (f - \mu)/\alpha$) and simplify,

$$\phi_\pm^4 + \left(2 - \frac{\mu}{f}\right)\varepsilon^2\phi_\pm^2 + \left(1 - \frac{\mu}{f}\right)\varepsilon^2 \approx 0 \qquad \text{(D6)}$$

which has solutions

$$\phi_\pm^2 = \varepsilon^2\left(\frac{\mu}{2f} - 1\right) \pm \frac{\varepsilon}{2f}\sqrt{\varepsilon^2(2f - \mu)^2 - 4f(f - \mu)}. \qquad \text{(D7)}$$

(Figure 3 shows that this approximation actually works well over a large range of λ values.)

The $\tilde{\mathscr{L}}(\lambda)$ and $\tilde{\mathscr{L}}(\lambda\varepsilon)$ coefficients give a linear system for g_+ and g_-:

$$\begin{pmatrix} \dfrac{\phi_+^2}{\phi_+^2-1} & \dfrac{\phi_-^2}{\phi_-^2-1} \\ \dfrac{\phi_+^2}{\phi_+^2-\varepsilon^2} & \dfrac{\phi_-^2}{\phi_-^2-\varepsilon^2} \end{pmatrix} \begin{pmatrix} g_+ \\ g_- \end{pmatrix} = \begin{pmatrix} -n \\ -n \end{pmatrix}. \tag{D8}$$

The solution is:

$$g_\pm = \frac{n}{\phi_\pm^2} \cdot \frac{(\phi_\pm^2-\varepsilon^2)(\phi_\pm^2-1)}{\phi_\mp^2-\phi_\pm^2}. \tag{D9}$$

The solution becomes complex if

$$\varepsilon^2 < \frac{4f(f-\mu)}{(\mu-2f)^2}; \tag{D10}$$

in this case the values of $\phi_\pm$ are complex, and the covariance becomes a damped sinusoid:

$$c^*(x) = \frac{\lambda}{2} e^{-\lambda\phi_r|x|}(g_r\cos(\phi_i\lambda|x|) + g_i\sin(\phi_i\lambda|x|)). \tag{D11}$$

The values of the scale parameters and coefficients can be derived by writing out the equilibrium covariance in terms of $g_\pm$ and $\phi_\pm$ (as a sum of complex exponentials) and then transforming to the sinusoidal form; the calculation is straightforward but tedious.

The scale parameters ϕ_r and ϕ_i are the real and imaginary parts of ϕ_+, which requires taking the complex square root of ϕ_+^2 (finding the solution to the equation $(\phi_r + i\phi_i)^2 = \phi_+^2$). The coefficients g_r and g_i are the coefficients of $\exp(\phi_r)$ and $\exp(\phi_i)$, and because g_+ and g_- are complex conjugates $g_r = 2\mathrm{Re}(g_+)$ and $g_i = 2\mathrm{Im}(g_+)$.

ACKNOWLEDGMENTS

We express our great appreciation to Simon Levin for suggesting the topic of moment closure in the first place, and for his subsequent guidance and useful suggestions in approaching this problem. Thanks go to Juan Lin for helpful conversations and for the suggestion of back-calculating parameters from the equilibrium distribution. In addition, we thank many other people who have helped with the development of these ideas, including Jonathan Dushoff, George Hurtt, Takuya Kubo, Mark Lewis, Paul Moorcroft, several anonymous reviewers, and Rick Durrett, whose comments helped improve the manuscript. We are pleased to acknowledge the support of NASA Grant NAGW-4688 to Stephen Pacala and Simon Levin.

REFERENCES

Atkinson, W. D., and Shorrocks, B. 1981. Competition on a divided and ephemeral resource: A simulation model, *J. Anim. Ecol.* **50**, 461–471.

Bartlett, M. 1956. Deterministic and stochastic models for recurrent epidemics, *in* "Proceedings of the Third Berkeley Symposium on Mathematical Statistics and Probability," Vol. 4, pp. 81–109, University of California Press, Berkeley.

Cain, M., Pacala, S., and Silander, J., Jr. 1991. Stochastic simulation of clonal growth in the tall goldenrod, *Solidago altissima*, *Oecologia* **88**, No. 4, 477–485.

Chesson, P., and Warner, R. 1981. Environmental variability promotes coexistence in lottery competitive systems, *Am. Nat.* **117**, 923–943.

Diggle, P. 1983. "Statistical Analysis of Spatial Point Patterns," Academic Press, New York.

Durrett, R., and Levin, S. 1994a. The importance of being discrete (and spatial), *Theor. Pop. Biol.* **46**, 363–394.

Durrett, R., and Levin, S. 1994b. Stochastic spatial models: a user's guide to ecological applications, *Philos. Trans. R. Soc. London B* **343**, 329–350.

Durrett, R., and Neuhauser, C. 1994. Particle systems and reaction-diffusion equations, *Ann. Probab.* **22**, No. 1, 289–333.

Ford, E., and Diggle, P. 1981. Competition for light in a plant monoculture modelled as a spatial stochastic process, *Ann. Botany* **48**, 481–500.

Gilpin, M., and Hanski, I. (Eds.) 1991. "Metapopulation Dynamics: Empirical and Theoretical Investigations," Academic Press, London.

Grenfell, B., Wilson, K., Isham, V., Boyd, H., and Dietz, K. 1995. Modeling patterns of parasite aggregation in natural populations: trichostrongylid nematode-ruminant interactions as a case study, *Parasitology* **111**, S135–S151.

Harada, Y., and Iwasa, Y. 1994. Lattice population dynamics for plants with dispersing seeds and vegetative propagation, *Res. Popul. Ecol.* **36**, No. 2, 237–249.

Harper, J., and White, J. 1974. The demography of plants, *Annu. Rev. Ecol. Syst.* 419–463.

Holmes, E., Lewis, M., Banks, J., and Veit, R. 1994. Partial differential equations in ecology: spatial interactions and population dynamics, *Ecology* **75**, No. 1, 17–29.

James, J. 1995. "A Student's Guide to Fourier Transforms with Applications in Physics and Engineering," Cambridge Univ. Press, Cambridge.

Levin, S. A., and Segel, L. A. 1982. Models of the influence of predation on aspect diversity in prey populations, *J. Math. Biol.* **14**, 253–284.

Lewis, M., and Pacala, S. 1997. Modeling and analysis of stochastic invasion processes. Submitted to *J. Math. Biol.*

Matsuda, H., Ogita, N., Sasaki, A., and Satō, K., 1992. Statistical mechanics of population: The lattice Lotka-Volterra model, *Prog. Theor. Phys.* **88**, No. 6, 1035–1049.

Mimura, M. 1981. Stationary pattern of some density-dependent diffusion system with competitive dynamics, *Hiroshima Math. J.* **11**, 621–635.

Mimura, M., Nishiura, Y., Tesei, A., and Tsujikawa, T. 1984. Coexistence problem for two competing species models with density-dependent diffusion, *Hiroshima Math. J.* **14**, 425–449.

Molofsky, J. 1994. Population dynamics and pattern formation in theoretical populations, *Ecology* **75**, No. 1, 30–39.

Murray, J. 1990. "Mathematical Biology," Biomathematics, Vol. 19, 2nd ed., Springer-Verlag, New York/Berlin.

Okubo, A. 1980. "Diffusion and Ecological Problems: Mathematical Models," Biomathematics, Vol. 10, Springer-Verlag, New York/Berlin.

Pacala, S. 1986. Neighborhood models of plant population dynamics. II. Multi-species models of annuals, *Theor. Popul. Biol.* **29**, 262–292.

Pacala, S., Canham, C., Saponara, J., Silander, J., Kobe, R., and Ribbens, E., 1996. Forest models defined by field measurements. II. Estimation, error analysis, and dynamics, *Ecol. Monographs* **66**, 1–44.

Pacala, S., and Silander, J., Jr. 1985. Neighborhood models of plant population dynamics. I. Single-species models of annuals, *Am. Nat.* **125**, 385–411.

Pacala, S., and Silander, J., Jr. 1987. Neighborhood interference among velvet leaf, *Abutilon theophrasti* and pigweed, *Amaranthus retroflexus*, *Oikos* **48**, 217–224.

Provencher, L., and Riechert, S. 1994. Model and field-test of prey control effects by spider assemblages, *Environ. Entomol.* **23**, No. 1, 1–17.

Real, L., Marschall, E., and Roche, B. 1992. Individual behavior and pollination ecology: implications for sexually transmitted plant diseases, *in* "Individual-Based Models and Approaches in Ecology" (D. DeAngelis and L. Gross, Eds.), pp. 492–510, Chapman and Hall, London.

Ripley, B. D. 1981. "Spatial Statistics," Wiley, New York.

Shmida, A., and Ellner, S. 1984. Coexistence of plant species with similar niches, *Vegetatio* **58**, 29–55.

Slatkin, M. 1973. Gene flow and selection in a cline, *Genetics* **75**, 733–756.

Solé, R., Bascompte, J., and Valls, J. 1992a. Stability and complexity of spatially extended two-species competition, *J. Theor. Biol.* **159**, 469–480.

Solé, R., Valls, J., and Bascompte, J. 1992b. Spiral waves, chaos and multiple attractors in lattice models of interacting populations, *Phys. Lett. A* **166**, 123–128.

Tilman, D. 1994. Competition and biodiversity in spatially structured habitats, *Ecology* **75**, No. 1, 2–16.

Urban, D., Bonan, G., Smith, T., and Shugart, H., 1991. Spatial applications of gap models, *For. Ecol. Manag.* **42**, No. 1/2, 95–110.

van den Bosch, F., Zadoks, J., and Metz, J. 1988. Focus expansion in plant disease. II. Realistic parameter-sparse models, *Phytopathology* **78**, No. 1, 59–64.

Whittle, P. 1957. On the use of the normal approximation in the treatment of stochastic processes, *J. R. Statist. Soc. B* **19**, 268.